# Microwave Heating of the Continuous Flow Catalytic Reactor in a Nonuniform Electric Field

**I. Plazl, G. Pipus, and T. Koloini**
Dept. of Chemical Engineering, University of Ljubljana, SLO-1001 Ljubljana, Slovenia

*Temperature profiles in the continuous-flow reactor with a fixed bed placed in a nonuniform microwave field are predicted by considering specific on–off regulation of the microwave power and local distribution of the electric-field intensity. The spatial and temperature dependence of the electric-field intensity affects the heating appreciably, as shown by indirect measurements. Results of numerical calculations agree with experimental data of outlet temperature and explain temperature oscillations in the outlet flow. The model developed allows an accurate description of microwave heating in the continuous-flow reactor associated with specific regulation of microwave power. The hydrolysis of sucrose catalyzed by the strongly acidic cation-exchange resin Amberlite 200C in R-H form was chosen as the reaction system. Calculated conversions of sucrose based on predicted temperature profiles agree with experimental data.*

## Introduction

Earlier findings that microwaves could be used to enhance specific chemical reactions have excited considerable research interest (Gedye et al., 1986; Giguere et al., 1986). Since then, the chemical applications have been extended to almost all areas of chemistry, and have consequently been the subject of a number of excellent reviews (Abramovitch, 1991; Mingos and Baghurst, 1991; Toma, 1993; Whittaker and Mingos, 1994). The advantages of microwave heating, such as selective direct heating of materials or a catalytic site, minimized fouling on hot surfaces, process simplicity, rapid startup, as well as the possibility of "dry" reactions and enhanced chemistry, demonstrate that many processes could be applied in the chemical and pharmaceutical industry.

The earliest reports of microwave organic reaction enhancement, using a commercially available microwave oven, were of reactions performed within closed PTFE vessels, which prevented the release of volatiles and avoided the risk of explosion. Many authors reported increases in reactions rates of up to $10^3$. This led to a debate about specific microwave effects on reactions. It is now recognized, however, that $10^3$-fold increases in reaction rate are due to the very high temperatures (over 100°C above the boiling point) achieved under high pressure (up to 50 atm). When reactions are performed at 1 atm, increases in reaction rates (if any) are less dramatic and can be attributed to local areas of superheating within the mixture.

Establishing the temperature effects has proved to be problematic, because of the difficulty of measuring the temperature accurately within a reaction mixture. Accurate measurement of the temperature within microwave cavities is an area of active research. Our previous report (Plazl et al., 1995) demonstrated a possible way of accurate temperature measurements within a standard microwave-heated laboratory stirred-tank reactor. The reactor was equipped with a glass cooling coil for maintaining constant temperature in the reactor during microwave heating, and with a specially designed NiCr-Ni thermocouple positioned in the reaction medium. We later designed a similar microwave reactor with reflux equipment, which allows one to carry out kinetic investigations either of low-boiling or polar high-boiling organic solvents under an improved control of reaction conditions (Plazl, 1994).

A major limitation of dielectric heating is the depth of penetration of the microwaves in an absorbing material. The use of continuous flow systems reduces the problems associated with penetration depth and sudden increases in pressure. However, many problems connected with microwave heating remain to be solved. These include expensive startup costs, monitoring of temperature, problems associated with control, and several variables in the heating rates (particle size, sam-

Correspondence concerning this article should be addressed to I. Plazl.

ple size, and geometry). The prediction of temperature profiles is essential for the design and efficient operation of chemical applications. The outlet temperature from continuous flow systems can be regulated by adjusting the flow rate and the power of the microwave oven. Kudra et al. (1989) reported that the outlet temperature oscillated at different power settings, except at the maximum power available. Power in the microwave oven is regulated by switching the magnetron off and on according to the duty cycle. As a result, the outlet temperature of a solution and the temperature profiles along the reactor oscillate with the same time period as the duty cycle of the microwave oven.

In this work, a mathematical model is developed to predict temperature profiles and sucrose conversion in a continuous-flow reactor placed in a nonuniform microwave field. Considering specific regulation of power, our model describes oscillation of the outlet temperature. Indirect measurements were performed to determine the spatial and temperature dependence of the electric-field intensity. The hydrolysis of sucrose was catalyzed by the strongly acidic cation-exchange resin Amberlite 200C in R-H form.

## Experimental Methods

The laboratory plant continuous-flow reactor was a Pyrex glass tube (1.07 cm ID), placed at full length (39 cm) in the axial position of the microwave oven. The microwave oven itself was a conventional unit (Panasonic NE-1780, Matsushita Electric Industrial Co., Osaka, Japan) that operated at a frequency of 2,450 MHz with adjustable power settings and with a full-power level of 1,700 W (four magnetrons). In addition, a continuous water-flow system with a total volume of 2,000 $cm^3$ was placed in the oven to absorb excess radiation and prevent magnetron damage. The temperature of the inlet and outlet flow was monitored with NiCr-Ni thermocouples. All data were gathered using a data-acquisition system (Burr-Brown Corp., Tucson, AZ). Before any experiments were performed with the microwave setup, the entire system was checked for leakage of microwaves. Details of the equipment are presented in Figure 1.

The temperature distribution along the fixed-bed reactor was measured indirectly by radiation thermometry with a thermal imaging system (Topscan 808, Fotona, Ljubljana, Slovenia; IR detector: Hg Cd Te; spectral range: 8–12 $\mu$m; and minimum temperature divisibility: 0.15°C at 30°C). It was assumed that water and glass emissivity were close to unity. After several minutes of steady state, the flow of the solution was interrupted, the microwave heating was stopped and the door was opened. The picture was immediately frozen and the point-to-point temperature of the reactor glass wall was determined.

The field intensity was determined by indirect measurements of the rate of temperature rise and the heating rate in the small "reactors" placed at different locations along the axial position of the microwave oven and at different initial temperatures. A small Plexiglas reactor (length = 25 mm; inner diameter = 10.7 mm) was filled with distilled water and with catalyst resins. It was placed separately at five different locations along the central axis of the microwave oven: $z = 0$ at the left side of the oven, $z = L/4$ at the left quarter of the oven, $z = L/2$ at the center of the oven, $z = 3L/4$ at the right quarter of the oven, and $z = L$ at the right side of the oven. In all cases, additional tubes with the same diameter and filled with water and a catalyst were placed on both sides of the reactor to keep the same geometry and volume as for the continuous-flow reactor. The microwave oven was run at full power for six to ten 6-s periods, between which the temperature in the reactor was measured by a NiCr-Ni thermocouple. The experiments were performed three times for location and for reactors with and without catalyst resins.

The hydrolysis of sucrose to fructose and glucose under catalysis by the strongly acidic cation-exchange resin Amberlite 200C in R-H form was chosen as the reaction system. In these experiments, the continuous-flow reactor was filled with

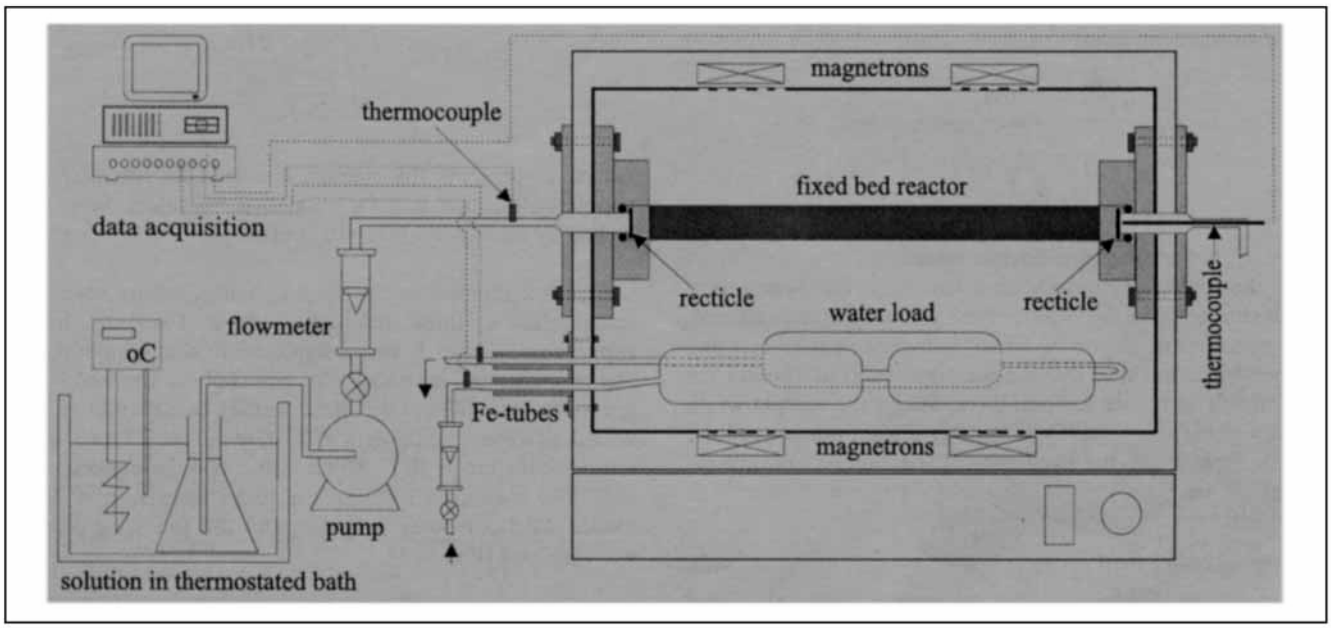


**Figure 1. Microwave heating: experimental setup.**

a catalyst (Amberlite 200C, Rohm & Haas, Deutschland, Frankfurt, Germany), 20% DVB, average particle size 0.82 mm, particle density 1,260 kg/m$^3$, moisture content 46–51%), and a wire mesh was placed at the ends of the reactor to prevent the loss of resin and to prevent the leakage of microwave irradiation. The microwave oven was run at half the maximum power until steady state was reached. The analysis of the samples was performed by the Knauer high-performance liquid chromatography (HPLC).

## Theory

A propagating electromagnetic wave is composed of oscillating electric ($E$) and magnetic ($H$)-field components. The power dissipated within the material is derived from Maxwell's equations of electromagnetic waves and leads to a simple expression involving the electric- and magnetic-field established in the material. If the magnetic effects are negligible, which is true for most materials used in microwave heating applications, the absorbed heat, $Q$, is determined by the following equation as shown by Metaxas and Meredith (1983):

$$Q = 2\pi f \epsilon_0 \kappa'' E^2, \tag{1}$$

where $E$ is the root-mean-squared (rms) value of the electric-field intensity. The frequency ($f$) of the microwaves is 2,450 MHz for most domestic ovens, $\epsilon_0$ is the dielectric constant of free space ($= 8.85 \cdot 10^{-12}\ \mathrm{AsV^{-1} \cdot m^{-1}}$) and $\kappa''$ is the relative-loss factor for the dielectric being heated, which at a given frequency is a function of the composition of the material and its temperature. For water (Metaxas and Meredith, 1983), it varies at 2,450 MHz as $320/T$ in the temperature range 25–75°C.

The dielectric constant and the loss factor determine the wavelength within the sample, the penetration depth, and the reflection coefficient. At 2,450 MHz, the wavelength in free space ($\lambda_0$) is 12.24 cm. The penetration depth, $D_p$, is the distance at which the incident electric field has decayed to $1/e$ of its incident level:

$$D_p = \frac{\lambda_0}{\pi\sqrt{2\kappa'}\sqrt{\sqrt{1+\left(\frac{\kappa'}{\kappa''}\right)^2}-1}}, \tag{2}$$

where $\kappa'$ is the relative dielectric constant.

As the dielectric constant and loss vary, the penetration depth changes and the electric field in the sample is altered. The penetration depth of water increases with increasing temperature, and thus the sample appears to be thinner for microwaves at higher temperatures. When the sample width is a few penetration depths or less, significant amounts of the electric field reach the back face of the sample and are reflected or lost.

### *Electromagnetic field*

The electric field inside the microwave oven has a very complex pattern. The intensity of the electric field inside a sample depends on several factors, including the dielectric constant and loss, the design of the oven, and the size and geometry of the sample. Because of the standing-wave pattern of the electric field, the spatial distribution of the field inside the cavity is fundamentally nonuniform. The electric field is zero at the position of the nodes, and no heat is generated in the sample at that location. At the antinodes, both the electric field and the rate of heat generation are at their maximum.

In our case, the continuous-flow reactor with a packed bed of porous resins (Amberlite 200C) as a catalyst was placed at full length in the axial position of the microwave oven. The reactor, together with the continuous-flow water load (with total volume of 2 dm$^3$) increases the complexity of electric-field distribution. The reactor size (inner diameter = 1.07 cm), the fluid-filled space outside and inside the solid particles, and the temperature differences between the inlet and outlet flow cause a considerable variation of the local electric-field intensity with the position and the temperature. In order to determine first the temperature profiles and then the concentration profiles in the continuous-flow reactor, the evaluation of local electric-field intensity is essential. In the absence of direct measurement or prediction, indirect measurements of field intensities are accomplished using the temperature rise in a small Plexiglas tube (same diameter as the reactor, 2.5 cm long). It was filled with water, with or without catalyst resins, and placed at the same location in the oven as the tubular reactor, but at different positions along the central axis (see the Experimental Methods section). Assuming that there are no temperature gradients in a small mass of water, its energy balance is given by the equation:

$$Q = \rho_l c_{P,l} \frac{dT_l}{dt}, \tag{3}$$

where the losses (convective, radiative, and evaporative) have been ignored. From the rate of temperature rise, the heating rate, $Q$, can be determined and equated to the electric field, $E$, using Eq. 1:

$$E = \sqrt{\frac{\rho_l c_{P,l} \frac{dT_l}{dt}}{2\pi f \epsilon_0 \kappa''}}. \tag{4}$$

Again, $E$ presents the average electric-field intensity at an appointed position and for a small temperature range, controlled by short periods (6–10 s) of magnetron running at full power.

Figure 2 shows how the electric-field intensity varies with temperature at three different positions. Evidently, for our experimental setup $E$ varies significantly with temperature at any position, and with location, especially at the lowest temperatures. In order to facilitate further calculations we converted all experimental data of $E$ (five different locations and temperature range 20°C–80°C) into a two-dimensional function. The measured results were fitted by using the *Mathematica 2.2.3* computer program, and the following equation was obtained (Figure 3):

$$E = (2{,}123 \pm 105) + 12.4 \cdot T_l + [(5.6 \cdot T_l - 135 \pm 25)\cos(4\pi z/L)] + [(2.0 \cdot T_l - 66 \pm 12)\sin(2\pi z/L)], \tag{5}$$

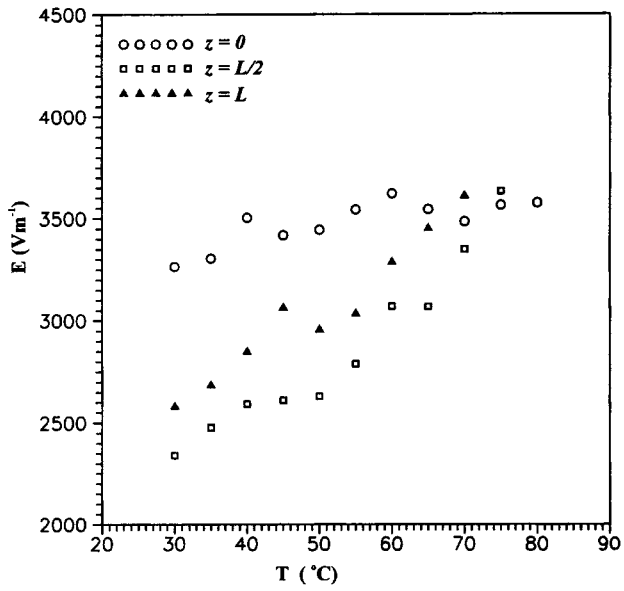


**Figure 2. Spatial and temperature dependence of electric-field intensity at three different locations in the fixed-bed reactor.**

where $T_l$ is the temperature of the liquid in degrees Celsius, $z$ is the dimensional variable, and $L$ is the length of the reactor. The experimental data were successfully covered by function with variation under $\pm 10\%$.

### *Mathematical model*

A mathematical model is proposed that describes the temperature and concentration profiles in a continuous-flow reactor with a fixed bed of catalyst in the stationary state. Considering the specific regulation of power, the model describes the oscillation of the outlet temperature. It is assumed that

- The flow in the bed is of the plug type (longitudinal dispersion is neglected)

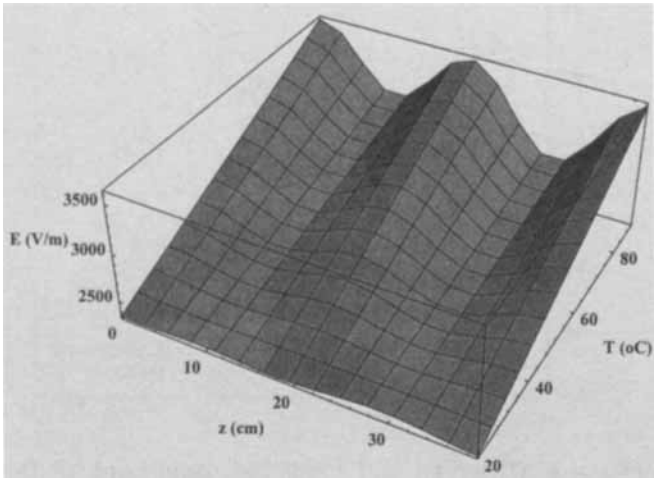


**Figure 3. Two-dimensional function of electric-field intensity.**

- There are no temperature and concentration gradients in the radial direction of the bed due to its small diameter
- The temperature inside the catalyst resin is uniform and the same as on the surface of the resin.

Applying these assumptions, the following equations are obtained:

*The Mass Balance for the Sucrose.* The hydrolysis of sucrose to fructose and glucose is the first-order reaction with respect to the concentration of sucrose (Plazl et al., 1995). The rate constant is given by the Arrhenius law:

$$\frac{\partial C}{\partial t} + v\frac{\partial C}{\partial z} = -k_0 e^{-(E_a/RT_l)}C. \tag{6}$$

*The Energy Balance for the Liquid.* The energy balance for the liquid includes heat transfer to the solid phase, heat transfer to the surroundings, and heat generation by the absorption of the microwave:

$$\epsilon_a \rho_l c_{P,l}\frac{\partial T_l}{\partial t} + \epsilon_a \rho_l c_{P,l} v\frac{\partial T_l}{\partial z} = (1-\epsilon_a)h_S a_S(T_S - T_l) + Ua_w(T_0 - T_l) + \epsilon_a 2\pi f \epsilon_0 \kappa'' E^2. \tag{7}$$

*The Energy Balance for the Solid Phase.* The energy balance for the solid phase includes heat transfer to the liquid phase and heat generated by the absorption of the microwave (moisture in the pores). Dry ion-exchange resins don't heat up under the microwave irradiation; however, the fluid-filled space outside and inside the solid particles couples with the microwave field and contributes to heating. Concentration of sucrose solution was small (10 $g \cdot L^{-1}$; 1 wt. %) and does not significantly affect the dielectric properties of water:

$$\rho_S c_{P,S}\frac{dT_S}{dt} = h_S a_S(T_l - T_S) + \epsilon_S 2\pi f \epsilon_0 \kappa'' E^2. \tag{8}$$

Associated initial conditions:

$$0 \le z \le L, \quad t = 0, \quad T_l = T_0 \quad T_S = T_0, \tag{9}$$

and boundary conditions at the inlet and the outlet of the reactor:

$$\begin{aligned} &z = 0, \quad t \ge 0, \quad C = C_0, \quad T_l = T_0 \\ &z = L, \quad t \ge 0, \quad \frac{\partial C}{\partial z} = 0, \quad \frac{\partial T_l}{\partial z} = 0. \end{aligned} \tag{10}$$

In Eqs. 6–10, $C$ is the concentration of sucrose; $E_a$ is the activation energy, $k_0$ is the preexponential factor; $T_l$ and $T_S$ are the temperatures of the liquid and solid phase; $\epsilon_a$ and $\epsilon_s$ are the void volume of the fixed bed and the porosity of the catalyst; $a_s$ and $a_w$ are the specific surface of the catalyst and the specific surface of the reactor wall, respectively; $U$ is the overall heat transfer coefficient; and $h_s$ is the heat-transfer coefficient between the liquid and the solid phase.

These balances are valid when the magnetron is turned on. When it is switched off, the same equations (Eqs. 6–10) are

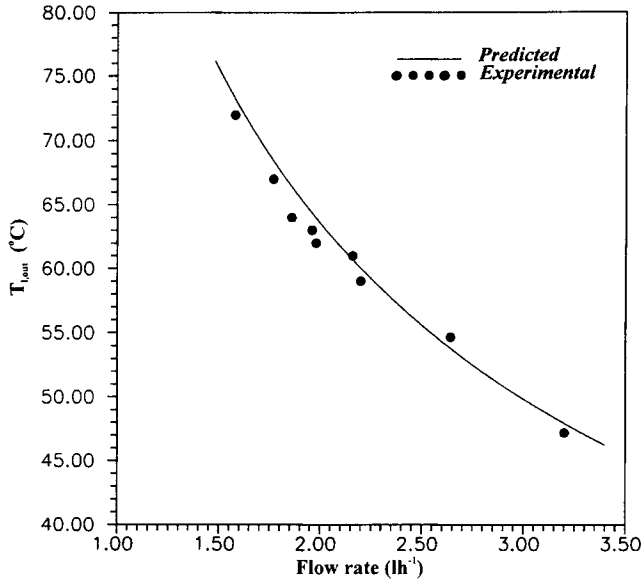


**Figure 4. Experimental and numerical data of outlet temperature at various flow rates.**

obtained but without the term for the heat generated due to the absorption of microwaves. The set of partial differential equations with associated initial and boundary conditions, together with the function for electric-field intensity (Eq. 5), was solved by the numerical method of finite differences.

## Results and Discussion

The comparison of the measured and calculated data of the outlet temperature and the conversion of the sucrose at various flow rates is shown in Figures 4 and 5, respectively. Both the measured and calculated data of the outlet temperature in Figure 4 present the time-averaged values of the temperature oscillations when the steady state is restored.

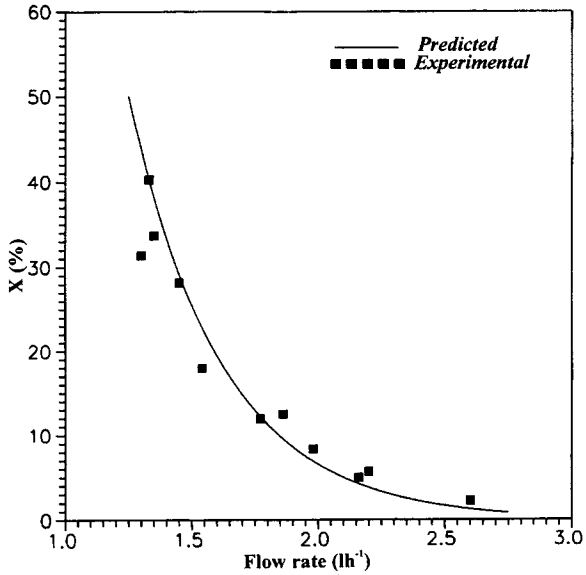


**Figure 5. Experimental and numerical data of conversion at various flow rates.**

Similarly, the sucrose conversions at the outlet of the reactor were calculated from the model and time averaged due to a duty cycle of 30 s. When the steady-state outlet average temperatures were reached, large enough samples were taken to calculate averaged conversion. The measured and calculated values of conversion are presented in Figure 5. In both cases (Figures 4 and 5), the regression errors were calculated at a 98% confidence level. The good agreement between the predicted and the measured values verified the mathematical model that is considering the spatial and temperature dependence of electric-field intensity (Eq. 5).

In order to avoid boiling as well as achieve the desired final temperature and the conversion of sucrose, all runs were performed with half the maximum available power, $P_0 = P_{max}/2$. The power in the microwave oven is regulated by switching the magnetron off and on according to the duty cycle. In our case, the duty cycle at half power is 30 s; the magnetrons (four magnetrons with a full-power level of 1,700 W) were run at full power for 15 s, and then they are switched off. Such cyclic irradiation causes oscillation of the temperature profiles along the reactor that can be observed in the oscillation of the outlet temperature even when the steady state is restored. Figures 6 and 7 illustrate the oscillations of the outlet temperature with the same time period as the duty cycle of the microwave oven. The numerical calculations are in agreement with the measured outlet temperatures in the $\pm 2$°C range. The model overpredicts the temperature rise of the outlet liquid at higher flow rates in Figure 7 for approximately 2°C, which is not the case at the lower flow rates (Figure 6). We assume that the underprediction of peak temperature in Figure 7 is probably due to the changes in the flow regime at the outlet of the reactor, where the thermocouple was placed. After the recticle, the reactor tube was contracted (inner diameter changed from 10.7 to 5.8 mm) (see Figure 1). This surely disturbs the flow pattern, which is more obvious at higher flow rates.

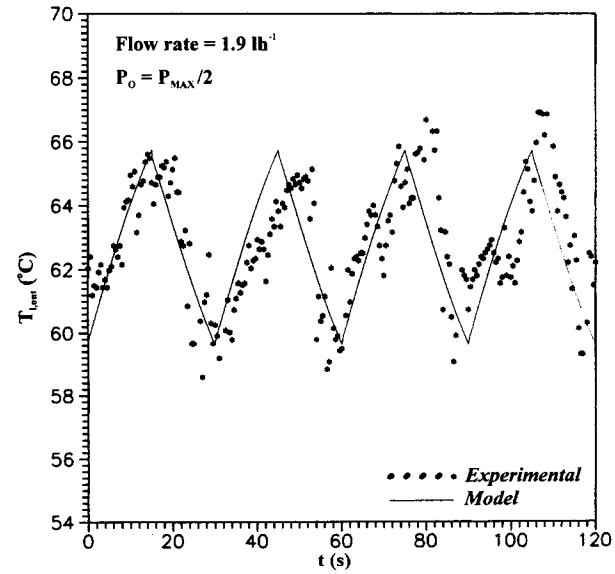


**Figure 6. Observed and predicted oscillations of the outlet temperature in quasi steady state (flow rate = 1.9 L·h$^{-1}$).**

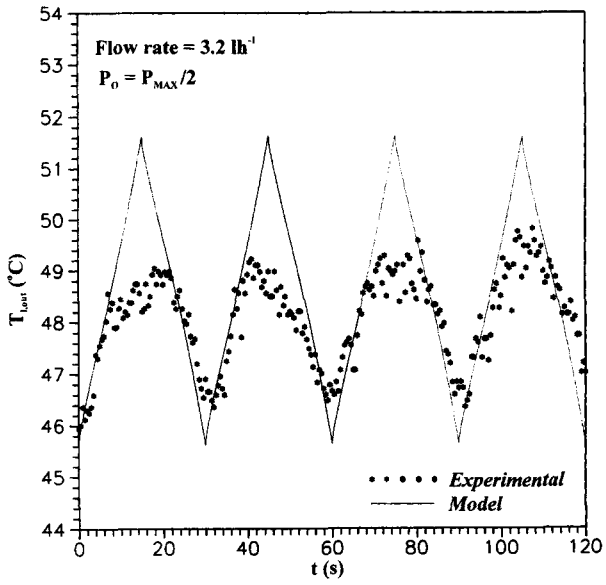


**Figure 7. Observed and predicted oscillations of the outlet temperature in quasi steady state (flow rate = 3.2 L·h$^{-1}$).**

The theoretical temperature profiles in the fixed-bed reactor at two different flow rates, predicted with the described model, are shown in Figures 8 and 9. When the steady state is reached and the average outlet temperature is stable (the temperature oscillates around the average value), the temperature profile in the reactor still varies periodically with time between two extremes. The first extreme is reached if the fluid enters the reactor at the same time that the magnetrons are switched on, and the second if it enters the reactor at the same time that the magnetrons are switched off. The temperature distributions along the reactor were measured indirectly by radiation thermometry with a thermal imaging system (see the experimental section), and good agreement can be observed with the numerical calculations.

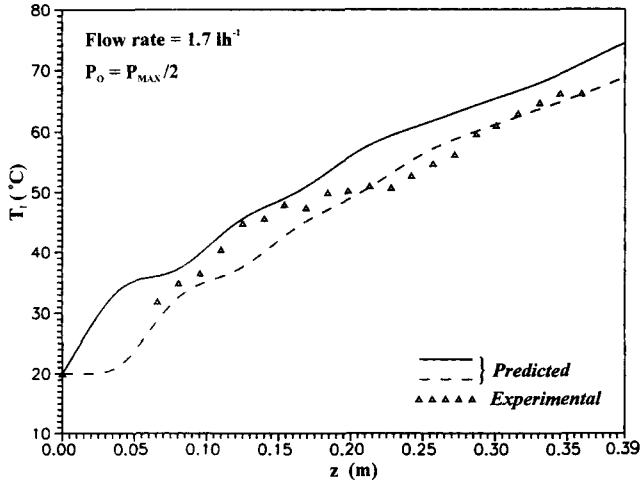


**Figure 8. Experimental and numerical temperature profiles in quasi steady state (flow rate = 1.7 L·h$^{-1}$); temperature profile in the reactor varies with time periodically between two extremes.**

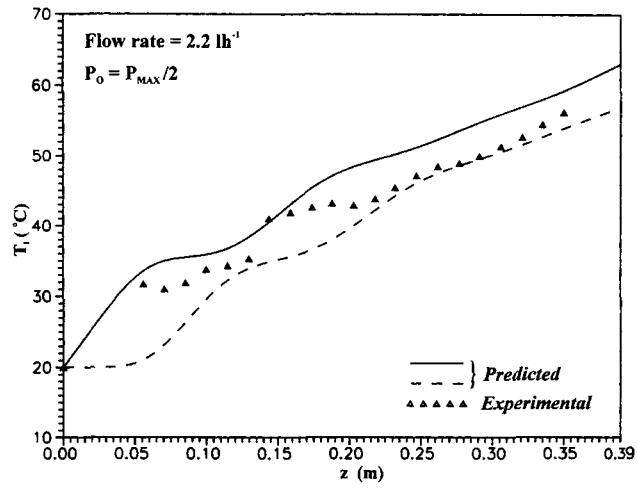


**Figure 9. Experimental and numerical temperature profiles in quasi steady state (flow rate = 2.2 L·h$^{-1}$); temperature profile in the reactor varies with time periodically between two extremes.**

Measured temperature profiles along the reactor clearly show that temperature profiles are affected by switching the magnetrons on and off. Temperature oscillations affect the conversion of sucrose. The mathematical model predicts that final conversion of sucrose also oscillates with the same time period and with a magnitude of 5%.

## Conclusion

Microwave heating of the continuous-flow reactor with a fixed bed placed in a nonuniform electric field was investigated. The absorbed microwave power and its spatial and temperature distribution in the reactor were determined experimentally and the numerical procedure was used in order to determine a two-dimensional function of the electric-field intensity.

The most convincing result of this study is the ability of the mathematical and numerical models to describe satisfactorily the temperature profiles in the continuous-flow reactor with a fixed bed of catalyst placed in a nonuniform electric field. These descriptions are also the basis for the prediction of reactant conversion.

The on–off regulation of the input power, also included in the mathematical model, is successfully confirmed by the observed and predicted oscillations of the outlet temperature and by the oscillations of the temperature profiles along the reactor, even when the quasi steady state is reached.

## Acknowledgments

The authors thank S. Gajšek, L. Prešeren, and M. Šmuc for their technical assistance.

## Notation

$c_p$ = specific heat capacity, J·kg$^{-1}$·K$^{-1}$
$L$ = reactor length, m
$R$ = gas constant, J·mol$^{-1}$·K$^{-1}$
$t$ = time, s
$T$ = temperature, K
$v$ = linear interstitial velocity, m·s$^{-1}$

$X$ = conversion of sucrose
$z$ = longitudinal distance, m
$\rho$ = specific density, $kg \cdot m^{-3}$

### *Subscripts*

$l$ = liquid phase
$s$ = solid phase
0 = initial values

## Literature Cited


Abramovitch, R., "Applications of Microwave-Energy in Organic-Chemistry—A Review," *Org. Prep. Proced. Int.*, **23**, 685 (1991).

Gedye, R., F. Smith, K. Westaway, H. Ali, L. Baldisera, L. Laberge, and J. Rousell, "The Use of Microwave Ovens for Rapid Organic Synthesis," *Tetrahedron Lett.*, **27**, 279 (1986).

Giguere, R. J., T. L. Bray, S. M. Duncan, and G. Majetich, "Application of Commercial Microwave Ovens to Organic Synthesis," *Tetrahedron Lett.*, **27**, 4945 (1986).

Kudra, T., H. S. Ramaswamy, G. S. V. Raghavan, and R. F. Van de Voort, "Microwave Heating for Pasteurization of Milk," ASAE Meeting (1989).

Metaxas, A. C., and R. J. Meredith, "Industrial Microwave Heating," *IEE Power Eng. Ser. 4*, Peter Peregrinus, London (1988).

Mingos, D. M. P., and D. R. Baghurst, "Applications of Microwave Dielectric Heating Effects to Synthetic Problems in Chemistry," *Chem. Soc. Rev.*, **20**, 1 (1991).

Plazl, I., "Esterification of Benzoic Acid by Conventional and Microwave Heating in Stirred Tank Reactor," *Acta Chim. Slovenica*, **41**, 437 (1994).

Plazl, I., S. Leskovsek, and T. Koloini, "Hydrolysis of Sucrose by Conventional and Microwave Heating in Stirred Tank Reactor," *Chem. Eng. J.*, **59**, 253 (1995).

Toma, S., "Use of Microwave Radiation in Organic Synthesis," *Chem. Listy*, **87**, 627 (1993).

Whittaker, A. G., and D. M. P. Mingos, "The Applications of Microwave Heating to Chemical Syntheses," *J. Microwave Power Electromagn. Energy*, **29**, 195 (1994).



*Manuscript received Apr. 17, 1996, and revision received Sept. 16, 1996.*